# Grafting of organic molecular precursors onto ZrC(100)//t-ZrO2(001) surfaces: When experimental and theoretical studies meet

Eric Osei-Agyemang, Arish Dasan, Romain Lucas, Sylvie Foucaud, Jean-François Paul, Sylvain Cristol, Etienne Laborde

# Grafting of Organic Molecular Precursors onto ZrC(100)//*t*-$ZrO_2$(001) surfaces: when Experimental and Theoretical Studies meet.

*Eric Osei-Agyemang,[1] Arish Dasan,[2] Romain Lucas,[2]* Sylvie Foucaud,[2] Jean-François Paul,[1] Sylvain Cristol,[1] Etienne Laborde[2]*

[1] Univ. Lille, CNRS, Centrale Lille, ENSCL, Univ. Artois, UMR 8181 - UCCS - Unité de Catalyse et Chimie du Solide, F-59000 Lille, France

[2] Univ. Limoges, CNRS, IRCER, UMR 7315, F-87000, Limoges, France

*to whom correspondence should be addressed: E-mail: romain.lucas@unilim.fr

**Keywords:** Grafting, DFT, atomistic thermodynamic modeling, functionalization, ZrC

---

**Abstract:** To control ZrC oxidation, one method is to coat the surface with SiC. This project therefore aims at grafting polymeric precursors on functionalized ZrC surfaces en-route to synthesizing ZrC/SiC core/shell composites. The exposed surface on the zirconia side of *t*-$ZrO_2$(001) (tetragonal $ZrO_2$) on top of a ZrC(100) substrate is first modified in presence of water. Water preferentially adsorbs molecularly and a subsequent functionalization with allylchlorodimethylsilane (ACDMS) in a $S_N$ reaction, appeared quite weak. However, the subsequent grafting of a repetitive unit of the polymeric precursor, built from diphenylsilane and 1,4-diethynylbenzene monomers through a hydrosilylation reaction, is a highly favorable and exothermic reaction. As the main problem occurs during the nucleophilic substitution reaction between ACDMS and hydroxyl groups on the surface, two bifunctional organic molecules, 3-

butenoic acid as well as glycolic acid, were also exploited. 3-butenoic acid adsorbed strongly to the Zr atoms of the surface, through chelating effects of the carboxylic acid group. The subsequent hydrosilylation reaction with a repetitive unit of the preceramic precursor was also a favorable exothermic reaction, indicating a promising approach for the grafting of organic macromolecules. In parallel, to associate experimental results, methyldiphenylsilane was grafted onto functionalized ZrC using 3-butenoic acid.

---

**1. Introduction**

Zirconium carbide (ZrC) is a non-oxide ceramic with a high melting point of ≈3400 °C. It exhibits excellent mechanical and physical properties. The presence of these properties are advantageous and as such, ZrC is used in several applications including the aerospace industry [1,2]. Another great advantage is the presence of an extremely high melting point. It is being considered in the nuclear industry as a structural and fission product barrier coating material for tri-isotropic (TRISO) coated nuclear fuel used in higher temperature reactors.[3] This makes it suitable for replacing or being used in addition to the currently

used ceramic silicon carbide (SiC, melting point of roughly 2700 °C).[4,5] Moreover, aside from the aforementioned excellent properties that make it applicable in a wide range of areas, a major setback is its easy oxidation. Thus, ZrC forms low refractory oxides (porous) at lower temperatures of 500-600 °C.[6] This problem is a serious difficulty in its numerous applications as the excellent physical and mechanical properties are deteriorated once it begins to oxide. The various accounts have been given on the oxidation at different conditions, and also on the various low index surfaces of ZrC. All studies have shown extremely strong interactions of oxygen with ZrC surfaces. Both theoretical and experimental analyses have been performed on the ZrC(111) surface.[7–11] All these studies showed a complete dissociation of oxygen into atomic species and its adsorption at three-fold hollow sites between three surface Zr atoms. On the ZrC(100) surface, several accounts have been given on the oxidation of this surface and all showed extreme reactivity of this surface with oxygen.[12–16] Oxygen dissociates completely into atomic species and adsorbs at an *mmc* site between two metals and one C atom on the surface. Only one theoretical report has been given on the oxidation of ZrC(110) surface, and the conclusion is a very exothermic dissociative adsorption oxygen leading to the final formation of a $ZrO_2$ layer on the ZrC surface.[7]

The nature of the oxide layer formed on the ZrC surface is not fully elucidated. A ZrO-like layer of $ZrO_x$ ($1 < x < 2$) has been observed on the ZrC surface.[13] The presence of this layer was observed to activate the ZrC(100) surface for further reaction with other molecules.[17] A separate study also reports the formation of a monolayer of oxygen atoms adsorbed on the ZrC(100) surface without any further diffusion of oxygen into the bulk ZrC, thus passivating the ZrC surface.[7] A similar feature was also observed for the ZrC(111) surface.[7] However, separate studies identified $ZrO_2$ as the oxide layer on ZrC and established crystallographic relationships between the ZrC and $ZrO_2$ facets that form the interface.[18,19] Several other experiments revealed $ZrO_2$ as the oxide phase formed on ZrC with the

appearance of cubic, tetragonal and monoclinic phases at different temperatures with the release of $CO_2$ gas.[20–25]

Aside from all the studies carried out on the oxidation of ZrC nanoparticles, no attempts have been made to control this oxidation and to maintain physical and mechanical properties that are required for the applications ZrC is known for. In this respect, it becomes imperative to develop a technique that provides protection from oxidation on ZrC surfaces. A viable method is to coat ZrC particles with SiC. Indeed, SiC forms protective oxide layers at higher temperatures of 1400 °C but does not oxidize at lower temperatures.

The conventional method in order to produce ZrC/SiC composites is to use conventional powders of SiC and ZrC, which are mixed and then sintered. The problem with this method is the heterogeneity of the sintered powders (*i.e.* densified materials). To control the composition and the structural homogeneity of the ceramics, the use of pre-ceramic precursors is a promising alternative.[26,27] SiC ceramics produced from polymeric precursors are known for their outstanding high temperature properties.[28,29] Thus, ZrC surfaces have to be modified first, to perform a grafting of the polymeric precursors in a second step, before pyrolysis of the hybrid objects (Figure 1).

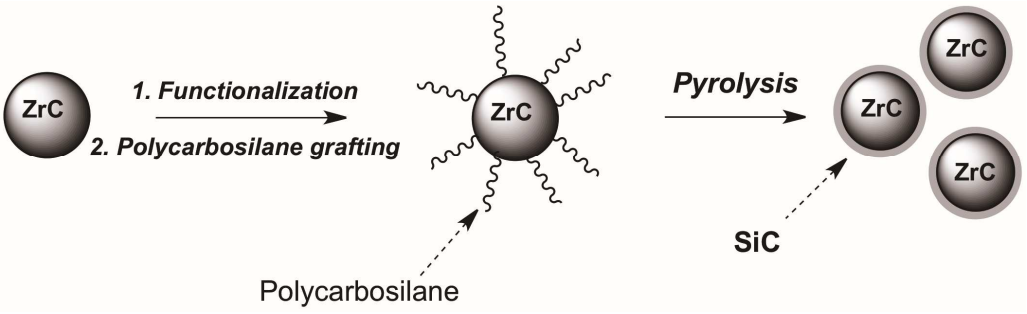


**Figure 1.** Scheme of the strategy to synthesize ZrC/SiC core/shell composites

However, there are only a few theoretical studies on the functionalization of ZrC with small molecules such as water or organic/organometallic compounds, described in the literature. For instance, the interaction of ZrC surfaces with water was recently described and led to the formation of hydroxyl groups onto the non-oxide ceramic.[30,31] Another contribution to the field revealed interactions between vinyl groups from polycarbosilanes and the metallic Zr in ZrC.[32] Thus, the exploitation of the affinity of vinyl groups of polyvinylsilanes on ZrC allowed for an improvement of the microstructural homogeneity in the resulting composites.[33] The nature of the bonds that developed between preceramic polymers on ZrC surfaces were, however, not investigated. The ability of the coating to be confined onto ZrC after a suitable pyrolysis will depend on the nature of the interactions of polycarbosilanes with ZrC surfaces. Surface modification and molecular grafting are crucial to control and must be properly characterized. This work aimed at providing new details on the efficiency of covalent polymer grafting on pre-functionalized ZrC particles, from both theoretical and experimental points of view.

The initial part of the manuscript considers an oxidized ZrC surface with *t*-$ZrO_2$. Then, the next part deals with the functionalization of the exposed $ZrO_2$ surface with water, using atomistic thermodynamics, further functionalization with allyl(chloro)dimethylsilane (ACDMS) and subsequent grafting of macromolecules SiC precursors. In the next section, the functionalization process of ZrC is initiated with carboxylic acids allowing for a further direct grafting of macromolecules. A final section gives conclusions and perspectives.

## 2. Experimental

### 2.1 Calculation schemes and methodology

#### 2.1.1 General Calculation Method

The Vienna Ab-initio Simulation Package (VASP)[34] based on Mermin's[35] finite temperature DFT was used for all calculations. The electronic configurations used for Zr, C, O, H and Si are $[Kr]4d^2 5s^2$, $[He]2s^2 2p^2$,

[He]$2s^2 2p^4$, $1s^1$ and [Ne]$3s^2 3p^2$, respectively. The core electrons as well as the core part of the valence electrons were represented with the Projector Augmented Wave-function (PAW) pseudo-potential in order to reduce the number of planewaves required for the description of the electronic wavefunction.[36] The generalized gradient approximation (GGA) as parametrized by Perdew, Burke and Ernzerhof (PBE) was used for the exchange correlation part of all calculations.[37] A Methfessel-Paxton smearing scheme was used by setting the gamma parameter to 0.1 eV and an optimized energy cut-off of 500 eV was used to expand the plane wave basis set in describing the valence electrons.[38] . A standard Mohkhorst-Pack special grid of 9 x 9 x 1 k-points was used for all surface calculations.[39] These parameters were defined in the study of the ZrC oxidation.[7] The self-consistent field (SCF) procedure for resolving the Kohn-Sham equations, convergence is assumed to be reached when two successive iterations have energy changes of $1 \times 10^{-4}$ eV. For all surface calculations, the positions of all the ions in the three top most layers were allowed to relax until the net forces acting on them were smaller than $10^{-2}$ eV/Å while keeping the bottom atoms fixed to mimic bulk properties.

For all surface calculations (1 x 1) unit cells were used except for lower coverage where larger surface supercells are considered. A vacuum of 12 Å is used to separate two periodically repeated slabs to prevent any unphysical surface-surface interactions. The slab used for all calculations is made up of a *t*-$ZrO_2$(001) (tetragonal $ZrO_2$) phase on top of a ZrC(100) substrate as shown in Figure 2. According to a previous experimental analysis, this slab configuration was selected. A preliminary analysis showed ZrC substrate thickness to have negligible influence on the adsorption properties of the exposed $ZrO_2$ surface and hence only two layers of ZrC were used as substrates.

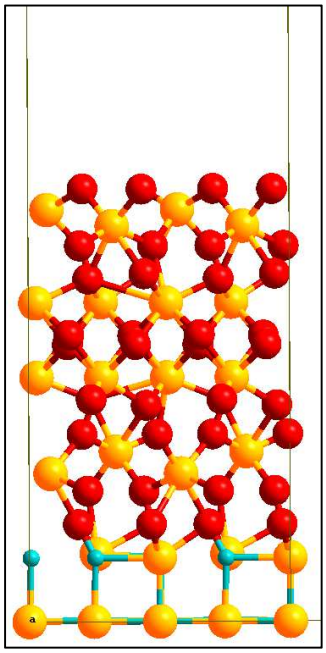

**Figure 2.** A (2 x 2) ZrC(100)/*t*-$ZrO_2$(001) slab. Color scheme: Red = O atoms, Yellow = Zr atoms, light blue = C atoms

The (1 x 1) cell lattice parameters are a=b= 4.736 Å and c=35 Å. The (1x1) cell exposed two oxygen and one zirconium atoms on the first layer and have an area of 22.433 $Å^2$.

Both molecular and dissociative adsorption modes were considered for adsorption and reactivity of molecules on the surface. The adsorption energy is calculated as in equation 1:

$$\boldsymbol{E_{ads} = -[E_{mol/Surf} - E_{Surface} - E_{mol}]} \quad \boldsymbol{eq.(1)}$$

In equation 1, $E_{mol/surf}$ is the DFT energy of the surface with adsorbed molecules on it, $E_{surface}$ is the energy of the free surface and $E_{mol}$ is the energy of the molecule in the gas phase. A positive adsorption energy means that the adsorption reaction is exothermic.

The effect of coverage is also investigated through the use of appropriate supercells to model coverages of 0.25 monolayer (ML), 0.50 ML, 0.75 ML and 1.0 ML. The coverage is determined by the ratio between

the water molecule and the surface oxygen atoms and such should be double for comparison with the number of accessible Zr atoms. A similar approach is used for further grafting of polymeric precursors on the functionalized surface.

2.1.2 Atomistic Thermodynamic Model

In order to provide a relationship between the 0 K calculated properties in DFT and experimentally relevant conditions, the already well-established atomistic thermodynamic model is used.[40] The assumption is that, the adsorbed molecules on the surface are in thermodynamic equilibrium with the gas phase serving as a reservoir for the gas phase molecules. We can then define a Gibbs free energy of adsorption ($\Delta_r G$) as a function of thermodynamic parameters like temperature, pressure and chemical potential through equation 2:

$$\Delta_r \boldsymbol{G} = \left[ \Delta \boldsymbol{E_O} + \Delta \boldsymbol{E_{ZPE(mol/surf)}} - \Delta \sum \boldsymbol{n\mu(T,\ p)} \right] \quad \boldsymbol{eq.(2)}$$

The zero-point energy (ZPE) contribution of the molecule upon adsorption on the surface is considered through the term $\Delta E_{ZPE(mol/surf)}$ while $\Delta E_O$ $(= -E_{ads})$ is the electronic energy difference between the surface with adsorbed molecules, the free surface and the free molecule in gas phase and is approximated by their respective DFT energies. $\Delta\mu\ (T,p)$ defines the difference in chemical potential of the gas phase molecules and all other released species in the reaction. Changes in the chemical potential of gas phase molecules contain temperature dependent terms as shown in equation 3:

$$\Delta \boldsymbol{\mu(T,P)} = \Delta \boldsymbol{\mu^o(T)} + \boldsymbol{RT} \ln\left(\frac{\boldsymbol{P}}{\boldsymbol{P^o}}\right) \quad \boldsymbol{eq.(3)}$$

Statistical thermodynamics is used to calculate the evolution of the chemical potential of the gas phase molecules due to the adsorption as follows:

$$\Delta\boldsymbol{\mu}^{\boldsymbol{o}}(\boldsymbol{T}) = \left[\boldsymbol{E}_{\boldsymbol{vib}(\boldsymbol{0}\rightarrow\boldsymbol{T})} + \boldsymbol{E}_{\boldsymbol{rot}} + \boldsymbol{E}_{\boldsymbol{trans}}\right] + \boldsymbol{RT} - \boldsymbol{T}(\boldsymbol{S}_{\boldsymbol{vib}} + \boldsymbol{S}_{\boldsymbol{rot}} + \boldsymbol{S}_{\boldsymbol{trans}}) \qquad \boldsymbol{eq}.(\boldsymbol{4})$$

These contributions can be obtained from standard statistical thermodynamic formulae through combination with calculated frequencies at equilibrium geometries. The values of $\Delta\mu^{o}(T)$ are calculated for the gas phase molecule at different temperatures. All contributions in the gas phase are considered while the adsorbed molecules are considered immobile with no rotational and translational degrees of freedom but only vibrational degrees of freedom. Thermodynamic stability plots are obtained at different temperatures and pressures with the calculated ($\Delta_r G$) values. The plots include effects of the different coverage.

2.2 Materials and measurements

Allylchlorotrimethylsilane (97%), 3-butenoic acid (96%), glycolic acid (95%), methyldiphenylsilane (97%), Platinum(0)-1,3-divinyl-1,1,3,3-tetramethyldisiloxane complex solution (Karstedt's catalyst), toluene (99.8%) and diethylether (99%) were obtained from Alfa Aesar. All the products were used as received. The ZrC used in this work was synthesized by a carbothermal reduction using a mixture of $ZrO_2$ (monoclinic, 99.5%, Alfa Aesar, Germany) and carbon (amorphous carbon black, 99.25%, Prolabo, France).[41] The starting powders of zirconia (15.6 g) and carbon (4.4 g) were mixed using a low speed planetary ball mill. Then the mixture was treated at 1750°C for 8 h in a graphite furnace (V.A.S. furnace, Suresnes, France) under flowing argon. The phase composition of the obtained powders was $ZrC_{0.96}O_{0.04}$ (04-002-5304), detected by X-ray diffraction (Siemens D5000, Germany) using Cu $K_\alpha$ radiation. To determine the grain size distribution of the zirconium carbide powder, laser granulometry analyses were performed (AccuPyc II 1340, Micro-metrics France S.A. Verneuil Halatte, France). The specific surface

area (SSA) of powders was measured thanks to the gas adsorption method (ASAP 2010, Micromeritics France S.A., Verneuil Halatte, France). Samples (600 mg) were degassed at 250°C for 12 h. Analyses were then carried out at 77 K under nitrogen (99.999%, Air liquide). The BET specific surface area was calculated from the nitrogen adsorption data in the relative pressure range from 0.05 to 0.30. The surface of the raw and functionalized ZrC was analyzed by X-ray photoelectron spectroscopy (XPS, Kratos Axis Ultra DLD spectrometer), using a monochromatic Al $K_\alpha$ source (1486,6 eV). All binding energy scales were charged referenced to the C 1S peak (285.0 eV) arising from surface contamination. The area analyzed was 300 µm × 700 µm. The pass energy was 20 eV for the high-resolution spectra and 160 eV for the surveys. Simultaneous TG/DTA-MS measurements were performed with a NETZSCH STA 449 F3 apparatus coupled with a gas analysis system (OMNISTAR) in a stream of argon at a heating rate of 10°C/min. In order to remove the oxygen content of the system three consecutive blank runs with a TG-sample holder and the same $Al_2O_3$ crucible were further used. In order to distinguish the evolved gaseous products, whether it comes out from background or not, the results were compared with the blank run. The Zeta-potential measurements were obtained using a Zetasizer Nano ZS instrument (DLS, Malvern). The samples were suspended in water (0.001 wt %, pH=7.0) and three consecutive measurements of 60 scans were recorded at 25°C for each experimental condition.

2.3 Synthesis

2.3.1 Functionalization of ZrC surface with organic molecules

1 g of as-synthesized ZrC core particles was dispersed in 10 mL of diethylether by sonication. In order to perform an efficient functionalization, the dispersion was treated with a large excess of (140 equiv., assuming a maximum of 10 OH per $nm^2$ onto the surface) organosilane or carboxylic acids, *i.e.* either allylchlorodimethylsilane (ACDMS), glycolic acid (GA) or 3-butenoic acid (BA) [43-45]. After 24 h at 20 °C, the mixture was separated by filtering and washing with diethylether 5 times, repeatedly. Finally, the resulting functionalized particles were dried at 100 °C for 1 h.

2.3.2 Reaction of functionalized ZrC-butenoic acid (FZrC-BA) with methyldiphenylsilane (MDPS)

A 50 mL round-bottom flask was charged with 1 g of FZrC-BA particles in 10 mL of toluene. Subsequently, 2 drops of Karstedt's catalyst were added into the suspension with magnetic stirring at room temperature for 10 minutes. Then, 0.69 mL of MDPS (140 equiv., assuming all the OH groups were functionalized by BA) in 10 mL of toluene were gradually added into the suspension. The hydrosilylation was performed with a constant stirring for 24 h at 75°C. After completion, the grafted particles were separated from the suspension by filtration and then washed several times by toluene and finally diethylether.

**3. Results and discussion**

3.1. Surface functionalization with $H_2O$: a theoretical approach

The initial study involved functionalizing the exposed surface with an appropriate molecule such as water. The use of water was motivated by the fact that, in our previous studies,[30,31] we achieved functionalizing the bare ZrC surfaces with water through the production of surface hydroxyl groups.

Considering both molecular and dissociative adsorption modes of water, the number of water molecules has been increased stepwise. The first water molecule was adsorbed in a dissociative mode with an OH

on top of Zr while the remaining H atom was adsorbed on an oxygen atom from the surface. The hydroxyl group was not bridged. The distance between a surface Zr and an O atom of the OH group is 2.11 Å while the surface O-H distance was 1.05 Å. The hydrated surface was further stabilized by hydrogen bonding between the OH group and the proton located on the surface as indicated by the large O-H distances. In order to form a bond with the hydroxyl group, the surface Zr atoms were displaced from their equilibrium position and relaxed upwards from their initial position. The adsorption energy for the first water molecule was 0.69 eV.

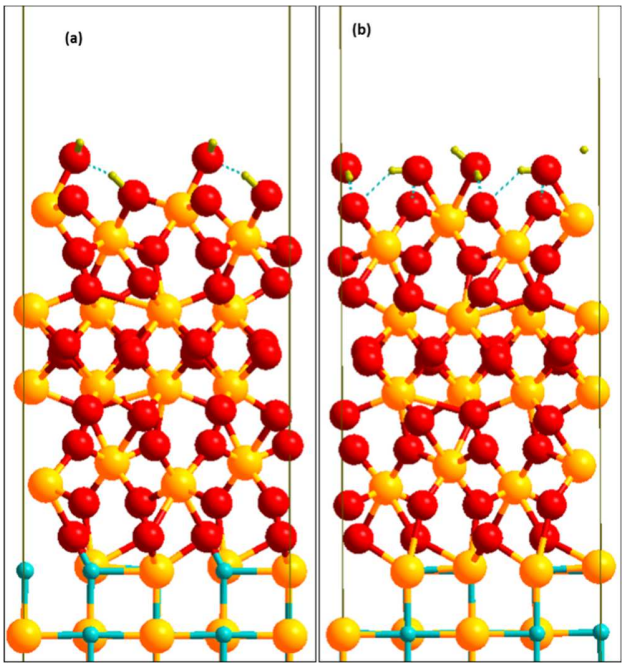


**Figure 3.** (2 x 1) ZrC(100)/*t*-$ZrO_2$(001) surface with adsorbed water molecules: (a) adsorption of 1 water molecule and (b) adsorption of 2 water molecules. Color scheme: red = O atoms, yellow = Zr atoms, light blue = C atoms, gold = H atom

The adsorption of a second water molecule was a molecular one. Furthermore, the adsorption of the second molecule leads to the displacement of the proton from the surface to the OH group restoring the 1$^{st}$ water molecule, to increase the hydrogen bond network, as indicated by the second adsorption (0.94

eV) that is larger than the 1st one. The equilibrium geometry first (0.5 ML) and second (1 ML) water molecules adsorbed on the surface are shown in Figure 3. There was an increase in bond distances between the surface Zr atom and O of the water molecules: 2.37 Å and 2.44 Å.

Intermediate coverages (0.25 ML and 0.75 ML) have been studied in a 2x1 supercell. The calculated adsorption energies at different coverages are provided in Table 1.

**Table 1.** Adsorption energies of water at different coverage on ZrC(100)/*t*-$ZrO_2$(001) exposed surface

| Coverage | 0.25 ML | 0.50 ML | 0.75 ML | 1.00 ML |
|---|---|---|---|---|
| Eads/eV/ $H_2O$ | 1.03 | 0.69 | 0.89 | 0.94 |

According to these results, the adsorption energies depend on the coverage. At 0.25 ML (dissociative adsorption) where there were almost no interactions with other hydroxyl groups, the adsorption energy is high. It decreased to reach a minimum of 0.50 ML for a dissociative adsorption. It began to increase again at a higher coverage due to the formation of the hydrogen bond network between the non-dissociated water molecules.

Figure 4 provides a density of states (DOS) plot for the adsorbed water on the surface. Figure 4 (top) shows a projected DOS for the surface atoms before adsorption of water molecules. The exposed surface is made up of $ZrO_2$ units. This $ZrO_2$ part presents a large gap between the conduction and valence bands. The metallic character of the system that can be seen in the insert (TDOS plot), is due to the ZrC support. However, the energy gap on the surface demonstrates that the conduction is localized in the support and that it does not modify the DOS on the surface. In parallel, the characteristic OH band in water was observed at -9.7 to -9.4 eV (Figure 4 bottom). Interactions of the water oxygen 2p with Zr (p and d) are localized in the [-6,-3] eV region demonstrating the covalent nature of the bonding.

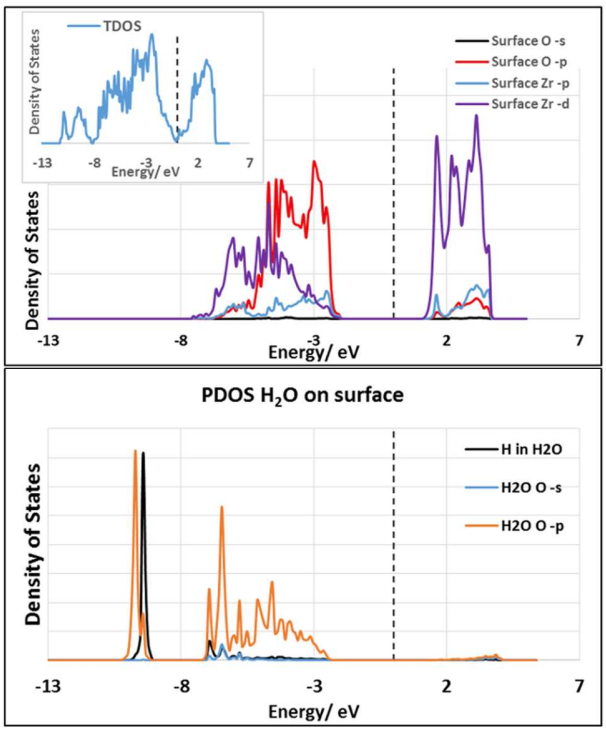


**Figure 4.** PDOS of surface (top) with TDOS of the exposed surface (insert of top figure), PDOS of $H_2O$ on exposed surface (bottom)

A thermodynamic treatment of the water molecule adsorption was also considered. The stability plot is given at three different temperatures by plotting the Gibbs free energy of the reaction $\Delta_r G$ against partial pressures of water at different coverages (Figure 5). The lowest line of such a plot is the most stable water coverage. The plots were presented at room temperature (298.15 K), 400 K and 500 K.

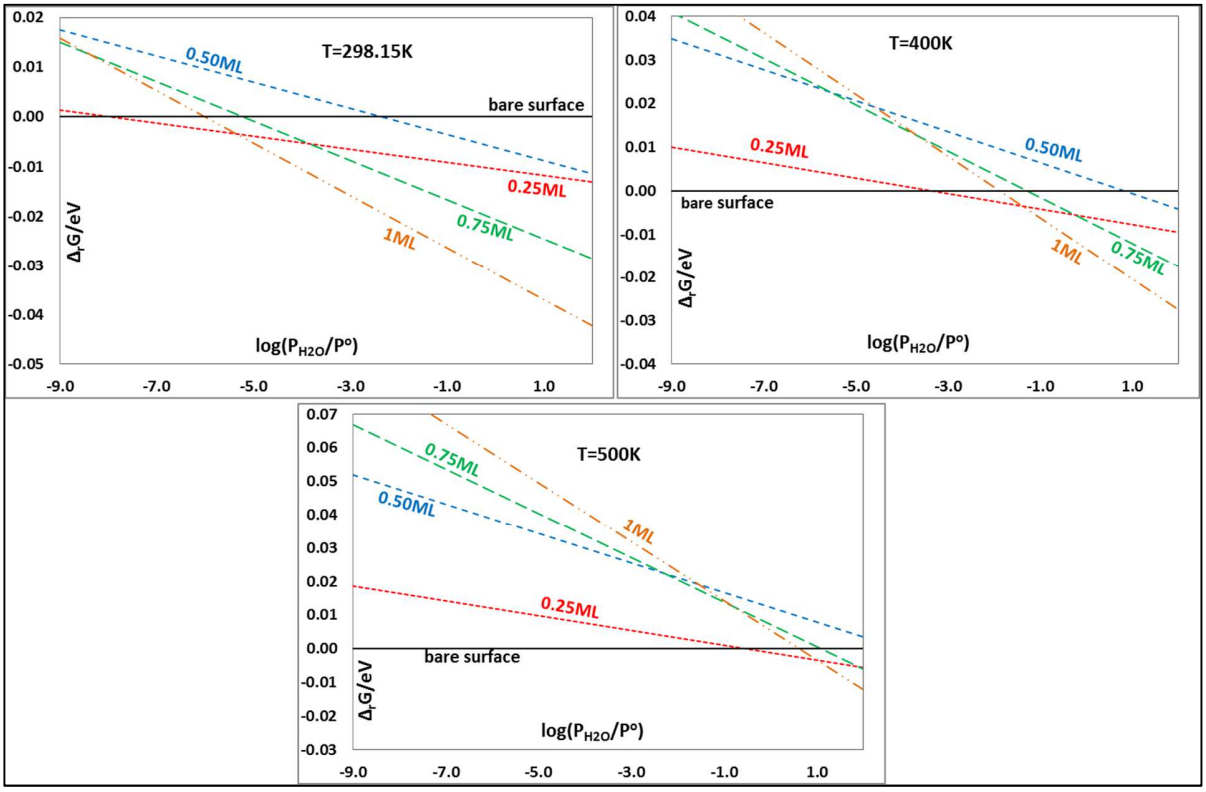


**Figure 5.** Stability plot for adsorption of water on ZrC(100)/*t*-$ZrO_2$(001) exposed surface

It is clear that at room temperature, the surface is fully covered by water at pressures higher than $10^{-5.5}$ bar. The bare surface is recovered at ultra-high vacuum pressures. It is noteworthy that the hydroxyl groups only present on the surface within $10^{-8}$ to $10^{-5.5}$ bar. The water molecules are easily removed from the surface as the temperature is increased. By increasing the temperature to 400 K, hydroxyl groups can be obtained within $10^{-3.5}$ to $10^{-1.5}$ bar. The nature of the surface is defined both by the temperature and the water partial pressure.

3.2 Functionalization with allyl(chloro)dimethylsilane: experimental and theoretical points of view

With the main aim of grafting a preceramic polymeric precursor on the surface, the next step is to further functionalize the surface with allyl(chloro)dimethylsilane (ACDMS).[42] This reaction is schemed in Figure 6. At this point, we used the fully hydrated surface for the functionalization with ACDMS. As demonstrated in Figure 5, this coverage is stable over a wide range of water partial pressures.

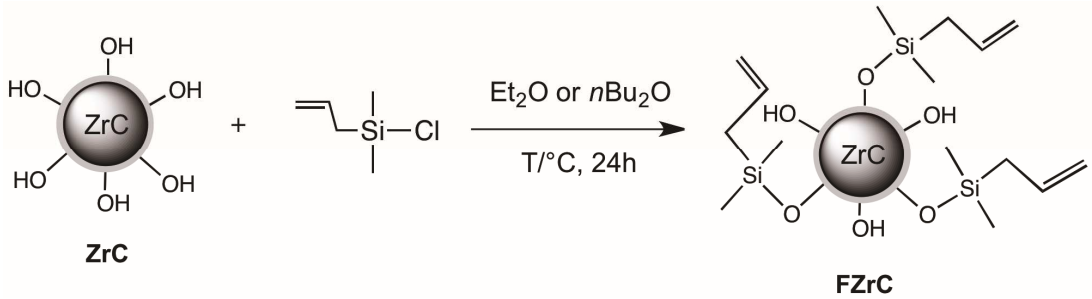


**Figure 6.** General procedure for the functionalization of deagglomerated ZrC with allyl(chloro)dimethylsilane (ACDMS) leading to functionalized ZrC (FZrC-ACDMS).[42] Visible OH groups represent a part of water molecules adsorbed on the surface.

Interaction of the hydrated surface with ACDMS is analyzed through calculation of the energy of the reaction. The reaction is considered to be a nucleophilic substitution with the release of HCl gas and leading to the presence of allyldimethylsilyl (ADMS) functional groups onto the surface (equation 5).

$$\mathbf{ZrC/ZrO_2—H_2O + ACDMS \rightarrow ZrC/ZrO_2—HO—ADMS + HCl} \qquad \mathbf{eq.\ (5)}$$

The calculated energy is -0.13 eV. This reaction energy shows that the process is not strongly exothermic. The starting point of the calculation was molecular water adsorbed on the surface on which the ACDMS was grafted. During the reaction one proton (from $H_2O$) moved to a surface O atom and ACDMS reacted with the resulting OH group in the nucleophilic substitution reaction. Thus, this

endothermic surface rearrangement contributed to the calculated total energy of -0.13 eV. Therefore, the functionalization with ACDMS was not a favored process and might not lead to a highly functionalized surface even if the departure of the gas HCl may displace the equilibrium in the forward direction. The resulting structure after the surface is functionalized with ACDMS, which is shown in Figure 7. The bond distance between O and Si (ACDMS) is 1.68 Å.

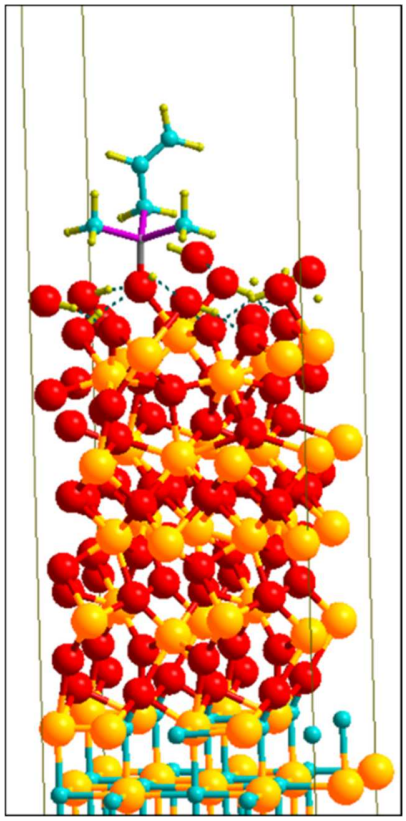

**Figure 7.** Hydrated ZrC(100)/*t*-$ZrO_2$(001) exposed surface modified with ADMS functional groups. Color scheme: Red = O atoms, Yellow = Zr atoms, light blue = C atoms, Gold = H atom, Grey = Si atom

An attempt to functionalize the ZrC surface with ACDMS was experimentally carried out via a nucleophilic substitution reaction In order to corroborate results from the theoretical approach.[42] To confirm the organic covalent grafting of obtained samples, XPS, TG/DTA-MS and zeta potential measurements were used. The survey spectra from XPS of a clean surface and a monomer grafted on the surface, are shown in Figure 8.

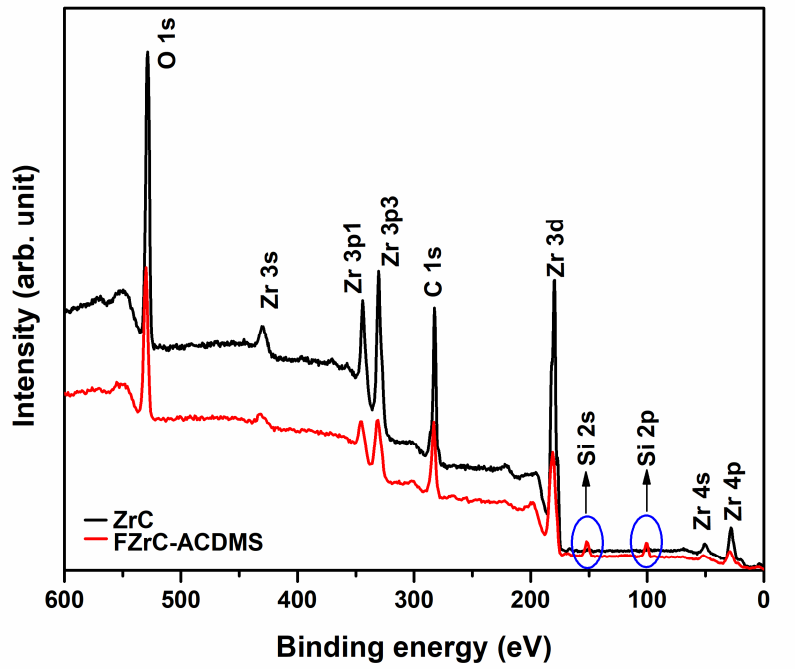


**Figure 8.** The full scan XPS survey for ZrC and FZrC-ACDMS

The survey spectrum clearly showed the presence of Si with a significant intensity, in addition to C, O and Zr contributions in the functionalized powder. This observation could be directly correlated with the grafting of the organosilane moiety onto the ZrO surface. To go further in the comprehension of the XPS results, deconvolutions of the high-resolution spectra were considered.

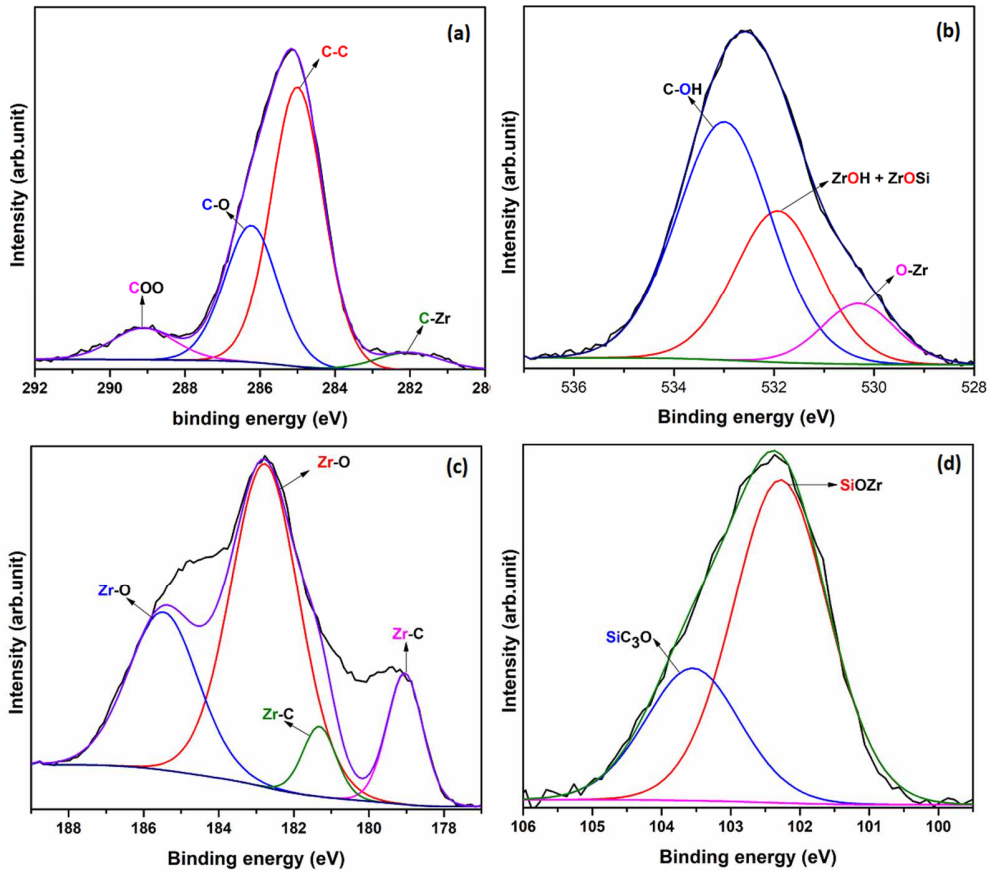


**Figure 9.** XPS profile of FZrC-ACDMS (a) C 1s (b) O 1s (c) Zr 3d and (d) Si 2p peaks

The deconvolution spectra of C 1s, O 1s and Zr 3d (Figure 9a-c) are composed of 4, 3 and 4 components, respectively. However, no significant chemical shifts were observed in comparison with the starting ZrC powders. Nevertheless, the deconvolution curves for Si (Figure 9d) can be fitted into two components respectively at 102.28 eV and 103.55 eV. The lower was attributed to a SiOZr environment and the more energetic could be correlated with a $SiC_3O$ environment.[42,43] Focusing on the elemental composition on the surface (Table 2) performed by XPS, the atomic concentration of oxygen and zirconium diminished (from 40.8 to 30.7 %, and from 12.3 to 7.2%, respectively), and the carbon content increased (from 46.9 to 57.2 %) after the functionalization leading to FZrC-ACDMS.

**Table 2.** Elemental composition (atomic percentage) performed by XPS on the particle surface for FZrC-ACDMS, in comparison with ZrC

| Sample | C (%) | O (%) | Zr (%) | Si (%) |
|---|---|---|---|---|
| **ZrC** | 46.9 | 40.8 | 12.3 | - |
| **FZrC-ACDMS** | 58.7 | 30.7 | 7.2 | 3.3 |

These results could be due to the attachment of a carbon enriched organosilane moiety. Moreover, no chlorine atoms were observed, which strongly supported that the attachment came through nucleophilic substitution reaction, and that the filtration was sufficient to remove impurities. In parallel, to confirm the success of the functionalization, TGA/DTA combined with quadrupole mass spectrometer tests were performed on both samples (raw and functionalized). Figure 10 shows TGA/DTA curves, with the corresponding gaseous species formed during thermal decomposition under argon flow. Even in such an atmosphere, the starting powders showed a slight weight loss by releasing carbon dioxide, followed by a slight increase in weight at 1000°C. This event is most likely attributed to the oxidation of ZrC then the weight decreased until 1400°C associated with the evolution of carbon dioxide as evidenced by corresponding mass spectra (Figure 10d). It is interesting to note that $H_2$ releases (m/z=2) around 600°C (Figure 10 b), were already proposed theoretically in a previous paper.[31] Indeed, oxygen modified ZrC can react with water molecules to form hydroxyl groups at the surface, and heating at higher temperatures can lead to the liberation of dihydrogen. The same phenomena were also observed for FZrC-ACDMS. Nevertheless, the initial weight loss and subsequent weight gain were more pronounced than the former.

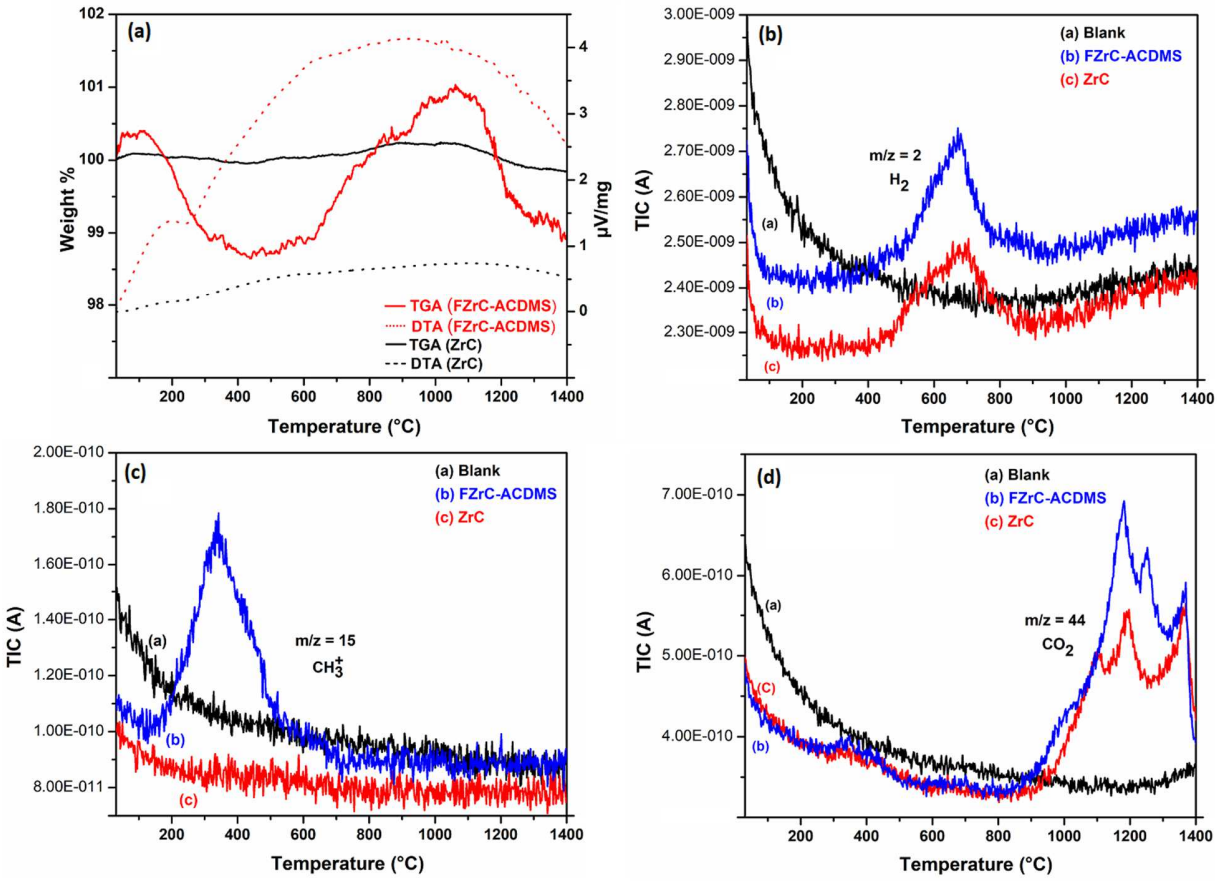


**Figure 10.** Simultaneous TG/DTA-MS base line corrected curves of (a) ZrC & FZrC-ACDMS; and gas evolution curves of various gaseous species: (b) hydrogen, (c) methyl ion, and (d) carbon dioxide

According to the mass spectrum of FZrC-ACDMS, new volatile species were found corresponding to m/z=15 around 380°C. This contribution was assigned to methyl ions, in addition to di-hydrogen (m/z=2) and carbon dioxide (m/z=44). This was an obvious confirmation of the presence of organosilane moiety on the surface of ZrC. Furthermore, the obtained zeta potential value of suspensions of FZrC-ACDMS (-26 mV) was higher than that of ZrC (-5 mV). It indicated more repulsive interactions between the particles than the starting powders,[44] proving the functionalization.

3.3 Grafting of preceramic precursor using grafting-to approach

To access hybrid core-shell systems, the next step was the grafting of a polycarbosilane precursor onto the functionalized surface.[42,45,46] To achieve this goal, a grafting-to approach was undertaken. In this route, an already synthesized macromolecule is covalently bonded to the functionalized surface (Figure 11).

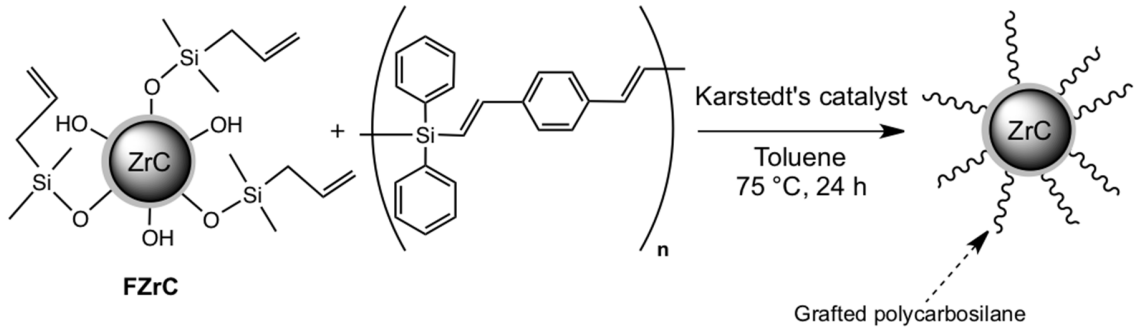


**Figure 11.** Grafting-to approach using a polycarbosilane precursor[42,45]

The macromolecule was synthesized from diphenylsilane and 1,4-diethynylbenzene monomers. Due to the grafting-to approach used in the synthesis, we decided to model the macromolecule as the monomer unit (*i.e.* $HSi(Ph)_2CH=CH-C_6H_4-CH=CH_2$). This reaction used the final Si-H bond of the macromolecule in a hydrosilylation reaction to attach the macromolecule to the alkene group of the allyldimethylsilane moiety on the modified surface. The energy of the reaction process was calculated using the monomer unit model. According to the results, the hydrosilylation reaction was theoretically observed to be a favorable exothermic reaction with a reaction energy of -0.79 eV. As such, the grafting-to approach will yield the desired grafted preceramic precursor on the modified surface, as it was experimentally demonstrated in a previous paper.[42] The grafted macromolecule through the grafting-to approach is shown in Figure 12.

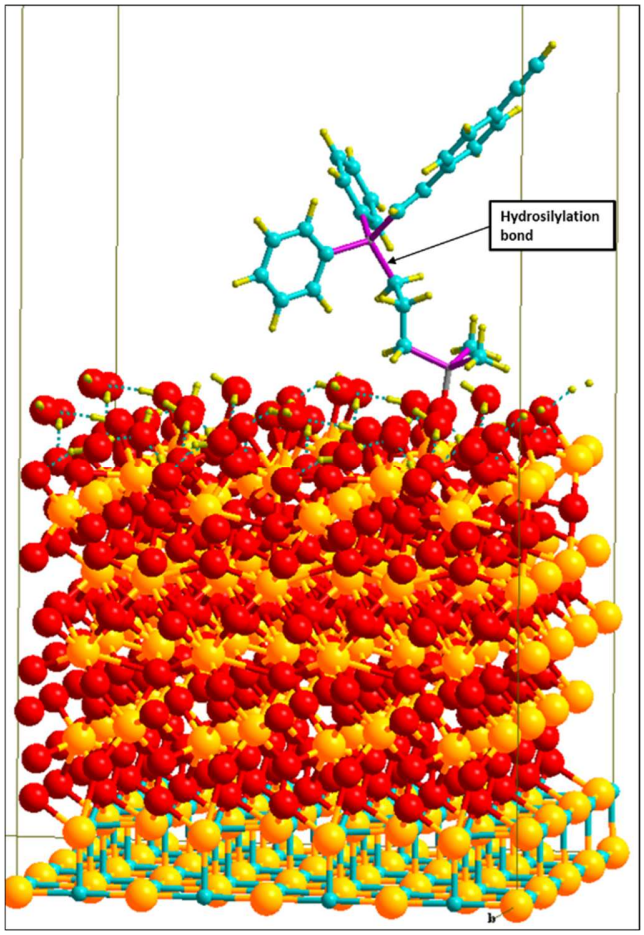


**Figure 12.** Grafted macromolecule through a hydrosilylation reaction. Color scheme:

Red = O atoms, Yellow = Zr atoms, light blue = C atoms, Gold = H atom, Grey = Si atom

The grafting of the macromolecule resulted in a blockage of several of the sites available in the vicinity of ADMS sites. The bond distance between Si of the grafted macromolecule and the terminal carbon ACDMS was 1.89 Å.

3.4 Functionalization with carboxylic acids

As noted in previous sections, there might be problems with the surface modification when water was used. Water will mainly exist as a molecular species and the functionalization with ACDMS is not a highly favorable reaction due to the low exothermic nature of the adsorption and its removal at low temperature. Another approach that could be considered was to explore bifunctional organic compounds such as carboxylic acid that can be used to modify the surface before the functionalization with ACDMS, in order to by-pass the hydration step. In light of this approach, several organic molecules were screened. These functionalizing molecules included both hydroxyl and carboxylic acid groups. Indeed, carboxylic acids could react with the surface of the ceramic and the hydroxyl functional group would then be free to react with ACDMS in a second step. To achieve this goal, the compounds that were initially considered and tested were small monofunctional (ethanoic acid) or bifunctional carboxylic acids: lactic acid, oxalic acid, ethanoic acid and 4-hydroxybenzoic acid (Figure 13).

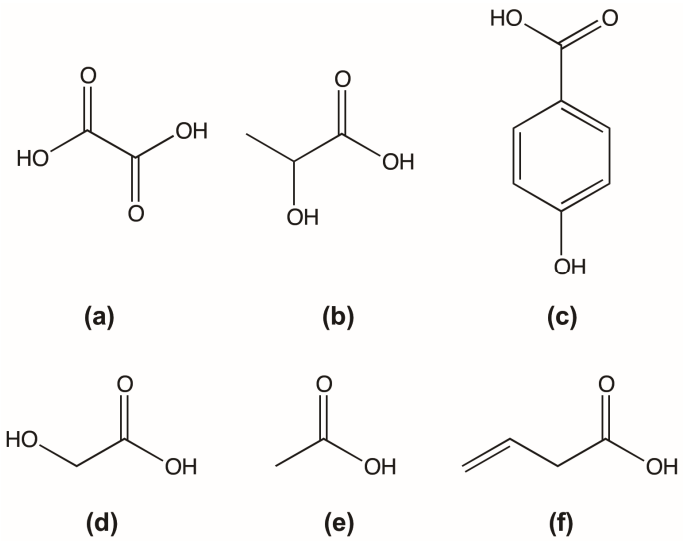


**Figure 13.** Carboxylic acids considered to functionalize the surface of ZrC: (a) oxalic acid, (b) lactic acid, (c) 4-hydroxybenzoic acid, (d) glycolic acid (GA), (e) ethanoic acid, (f) 3-butenoic acid (BA)

According to the theoretical results of calculated adsorption energies for the five different molecules (Table 3), all the compounds exhibited a strong interaction with the exposed surface through the carboxylic acid groups. We explored the adsorption through one O atom of the carboxylic acid group and the chelating effect of the two oxygen atoms. The chelating groups exhibited stronger interactions with surface Zr atoms with a protonation of surface O atoms.

**Table 3.** Adsorption energies for chelating group of different bifunctional organic molecules

| **Organic molecule** | **Oxalic acid** | **Lactic acid** | **Ethanoic acid** | **4-hydroxybenzoic acid** | **Glycolic acid (GA)** |
|---|---|---|---|---|---|
| **$E_{ads}$ (eV/ molecule)** | 1.26 | 0.99 | 1.03 | 0.84 | 1.28 |
| **ΔrE (Next nucleophilic substitution reaction with ACDMS)** | +0.58 | +0.40 | - | +0.15 | +0.95 |

To compare these results to experimental data, glycolic acid (GA) was selected, as it led to the strongest interaction with the exposed surface. The functionalization protocol was similar to the procedure used for the reaction of ACDMS with ZrC in toluene. To access the surface composition of the modified surfaces, XPS analyses were considered (Figure 14).

**Table 4.** Elemental composition (atomic percentage) performed by XPS on the particle surface for different FZrC, in comparison with ZrC

| Sample | C (%) | O (%) | Zr (%) | Si (%) |
|---|---|---|---|---|
| **ZrC** | 46.9 | 40.8 | 12.3 | - |
| **FZrC-GA** | 51.6 | 38.5 | 8.0 | - |
| **FZrC-BA** | 58.7 | 31.6 | 9.5 | - |
| **FZrC-BA+MDPS** | 66.3 | 26.7 | 2.9 | 4.2 |

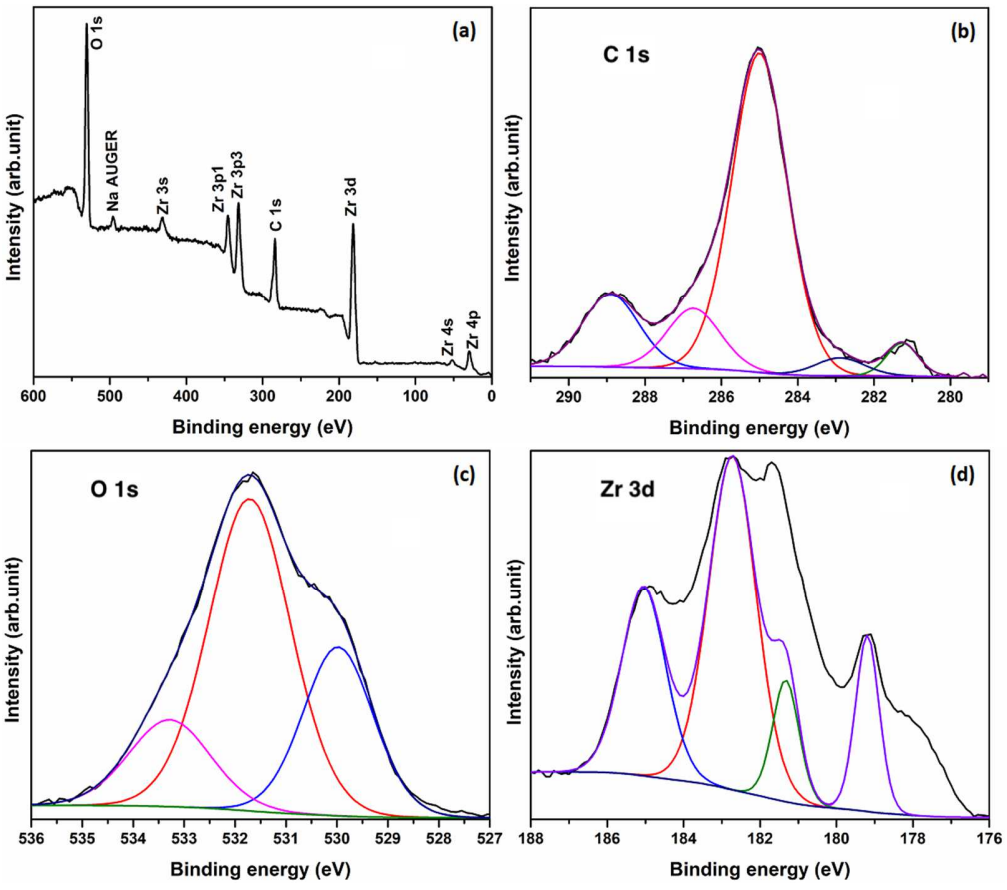


**Figure 14.** XPS for FZrC-GA (a) survey spectrum; (b) C 1s; (c) O 1s; (d) Zr 3d

First, the survey spectrum showed that the sample surface was mainly composed of C, O, Zr elements (Figure 14a). A minor contamination of Na was detected, which was likely due to the presence of Na in glycolic acid. Although the deconvolution curves (C 1s, O 1s and Zr 3d, Figure 14b-d) were similar to the analysis of starting powders, it can be observed from the elemental composition on the surface that Zr concentration was slightly reduced (8.0 %), carbon value increased (51.6 %) while the oxygen content (38.5 %) remained almost constant (Table 4). These observations could definitely be attributed to the ZrC surface coverage with glycolic acid molecules. In addition, to confirm these results, the thermal decomposition of the hybrid objects was observed with a particular attention paid to the released gaseous species during the treatment (Figure 15).

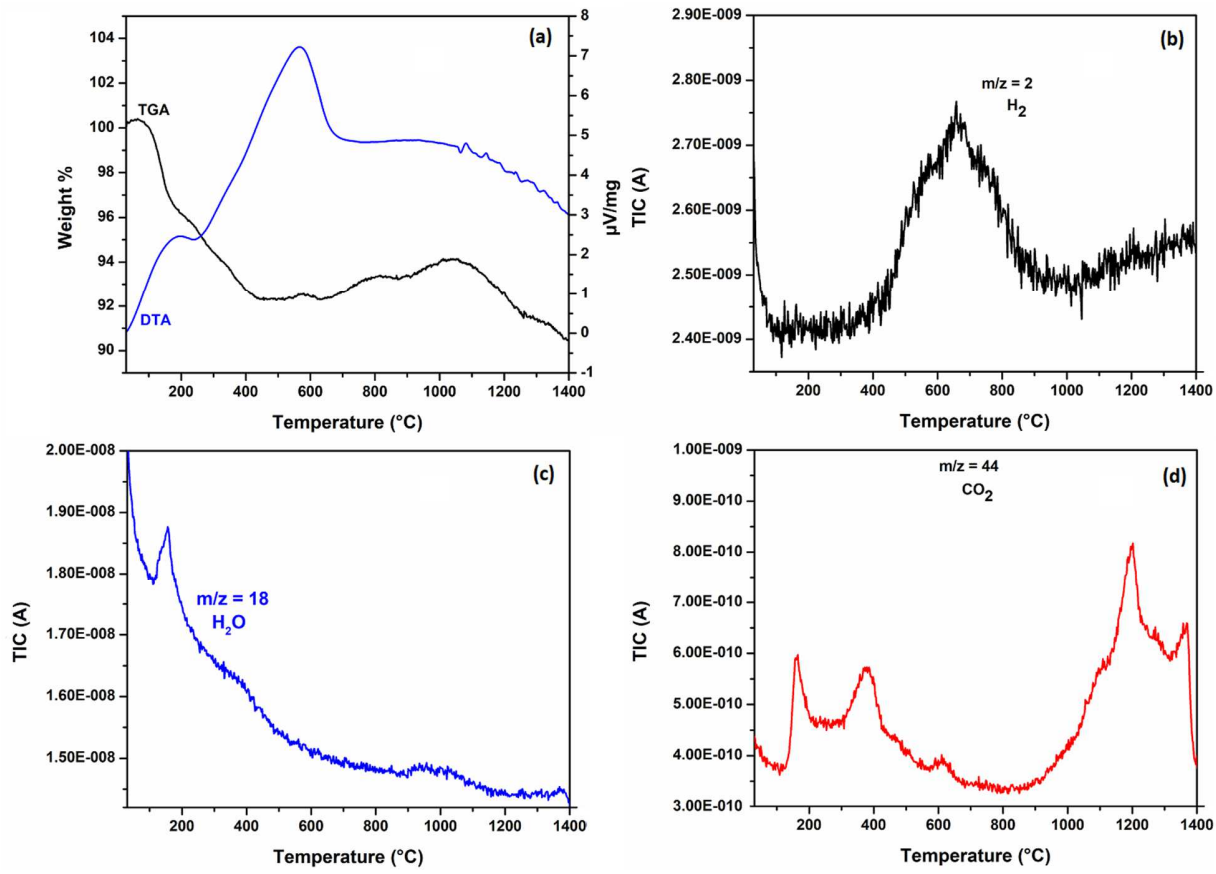


**Figure 15.** Thermal decomposition pattern of FZrC-GA (a) base line corrected TG-DTA curves, and gas evolution curves of various gaseous species (b) hydrogen, (c) water & iv) carbon dioxide

As can be seen in Figure 15a, the weight loss occurred from 110 to 400°C. In this temperature range, two stages of mass loss were identified. The first quick mass loss (~3 %) observed between 110 and 130°C was related to water (Figure 15c) and glycolic acid (bp = 100°C) molecules. This step was followed by ~5 % weight loss detected between 150 and 400°C. This event could be attributed to the decomposition of the organic molecules attached to the surface of ZrC. Different gaseous species ($H_2O$ and $CO_2$) were evidenced on this temperature range according to the corresponding mass spectra (Figure 15c and 15d). Interestingly, it was noticed that the $CO_2$ evolution occurred in three steps (Figure 15d). The sharp evolution in the very early period (155°C), was believed to be caused by the decomposition of glycolic acid attached onto the core surface.[47] Again, a higher zeta potential value of -25 mV showed more repulsive interactions between the particles than in the case of the starting powder, proving a change onto the surface of ZrC powders. Thus, these experimental results on the functionalization with glycolic acid were in good agreement with theoretical calculations, which yielded an adsorption energy of 1.28 eV through the carboxylic acid group (Table 3).

Following the functionalization of the surface with a pendant hydroxyl functional group, a further modification of the modified ZrC surfaces with ACDMS was tested in a nucleophilic substitution reaction (Table 3). The reactions between ACDMS and the considered hydroxyl groups generated on the surface, were all endothermic with values between 0.15 and 0.95 eV/molecule (Table 3). It therefore became obvious that the nucleophilic substitution reaction involving ACDMS, and hydroxyl functional groups did not seem appropriate for further grafting.

From this point of view, it was necessary to consider bypassing the nucleophilic substitution reaction of ACDMS by employing an organic bifunctional reagent that could be adsorbed directly onto the exposed surface, while exploring the other alkene functional group in the “grafting-to” approach in order to graft macromolecules.

3.5 Functionalization with 3-butenoic acid and further grafting of a “macromolecule model”

As discussed in the previous section, there was a need to consider different functional groups for the functionalization step. For the purpose of the work, 3-butenoic acid was selected as a good candidate: indeed, in the same molecule, an available carboxylic acid was present for an adsorption onto the exposed surface, and an available double bond could then be used for the next hydrosilylation reaction in the “grafting-to” approach. The calculated adsorption energy for 3-butenoic acid on the exposed surface using the chelating properties of the carboxylic acid group was of 1.00 eV. It indicated a strong interaction with surface Zr atoms through two O atoms of the organic molecule (Figure 16). The calculated bond distances between the surface Zr atom and the chelating O atoms were 2.35 Å and 2.32 Å.

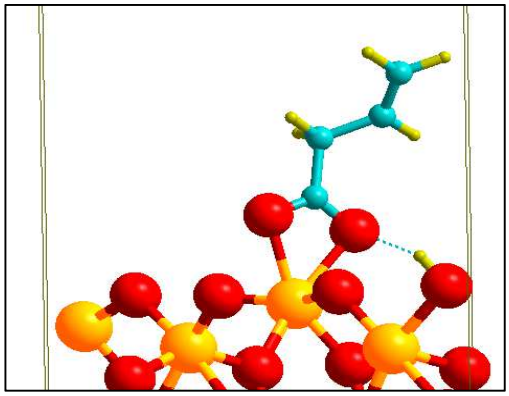

**Figure 16.** Adsorption of 3-butenoic acid on ZrC(100)/*t*-$ZrO_2$(001) exposed surface. Color scheme: Red = O atoms, Yellow = Zr atoms, light blue = C atoms, Gold = H atom

Focusing on the density of states (Figure 17), a plot was obtained for the adsorbed 3-butenoic acid on the surface in order to check the electronic structure. The DOS showed the bonding between O atoms of the chelating group in 3-butenoic acid and Zr atoms on the exposed surface. The bond was typically of Zr

–d mixing with O –p between -6.4 eV and -7.4 eV while the interaction with the Zr-p orbitals was located around -3 eV.

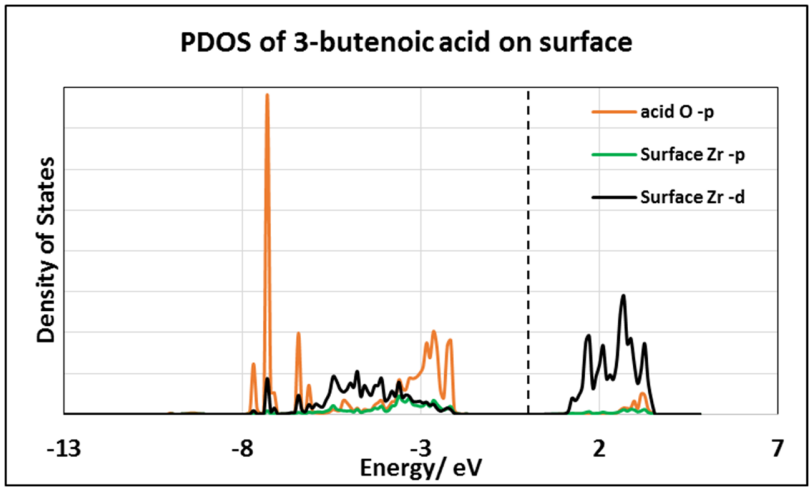


**Figure 17.** PDOS of 3-butenoic acid on ZrC(100)/*t*-$ZrO_2$(001) showing bonding with the surface

After a functionalization with 3-butenoic acid, the grafting-to approach was used to graft the preceramic macromolecules as described before, by utilizing the double bond of 3-butenoic acid for the hydrosilylation reaction. This reaction was highly favorable as observed in section 3.3 when the hydrosilylation reaction was carried out through the use of ACDMS. The calculated reaction energy for the hydrosilylation reaction was of -0.94 eV showing a favorable reaction.

Additionally, instead of using the monomer unit obtained from diphenylsilane and 1,4-diethynylbenzene, methyldiphenylsilane (MDPS, $CH_3SiH(Ph)_2$) was used for the hydrosilylation reaction after functionalizing with the ZrC surface with 3-butenoic acid, in order to simplify the system used, and to compare it with the experimental data. The calculated reaction energy for the hydrosilylation reaction using MDPS as the macromolecule was -1.08 eV indicating a highly exothermic process. It could be concluded that the use of MDPS would give a slightly more favorable hydrosilylation reaction than the macromolecule obtained from diphenylsilane and 1,4-diethynylbenzene monomer units.

For the experimental procedure, in the first step, 3-butenoic acid (BA) was attached to the surface of ZrC and then followed by a hydrosilylation reaction with MDPS, as a representative monomer unit in solution. To verify the functionalization and further grafting, XPS spectra for BA modified ZrC (FZrC-BA) and grafted surfaces (FZrC-BA+MDPS) were obtained (Figures 18 and 19).

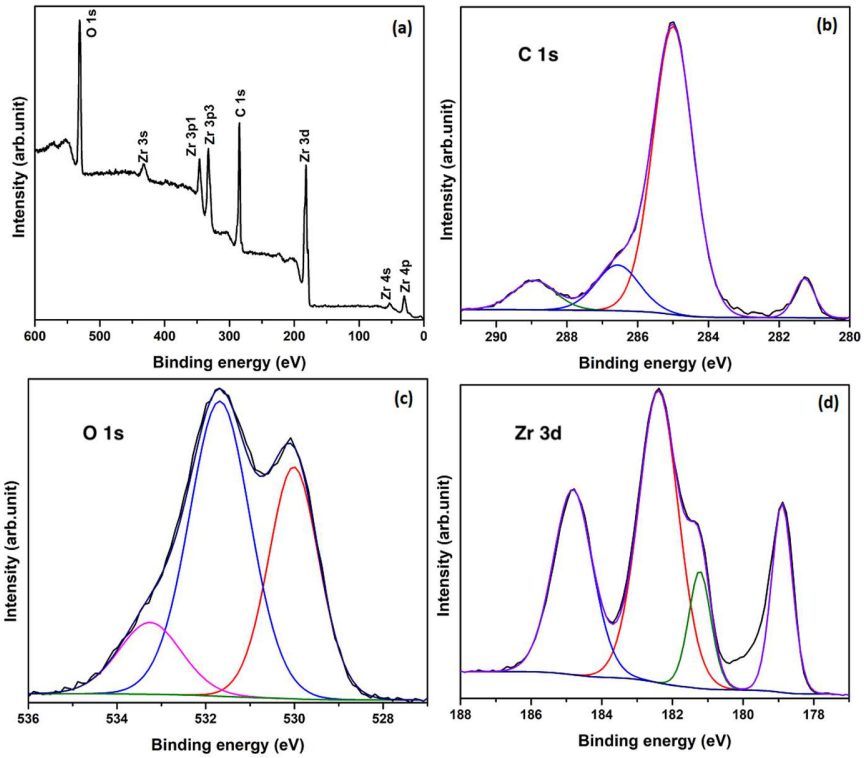


**Figure 18.** XPS for FZrC-BA (a) survey spectra; (b) C 1s; (c) O 1s; and (d) Zr 3d

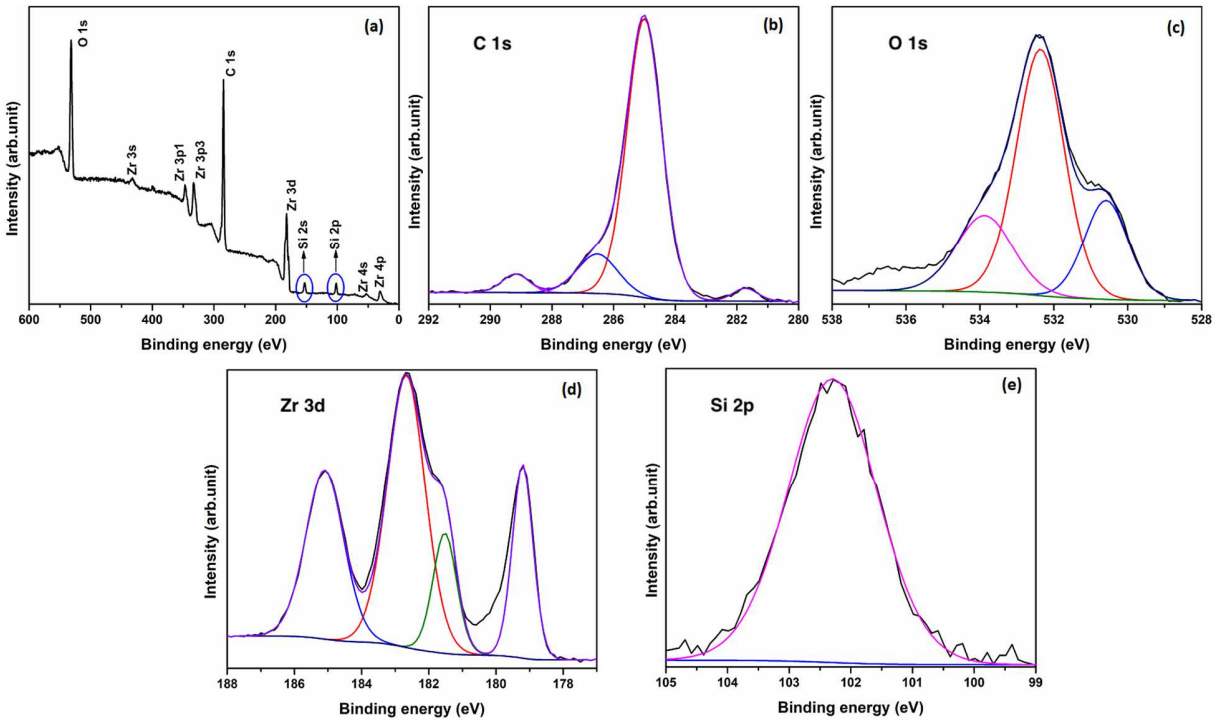


**Figure 19.** XPS for FZrC-BA+MDPS (a) survey spectra; (b) C 1s; (c) O 1s; (d) Zr 3d; and Si 2p

First, the presence of silicon in FZrC-BA+MDPS samples was clearly identified by the corresponding survey XPS spectrum (Figure 19a). All other spectra and binding energies obtained (Figures 18 and 19) were similar to those explained previously (Figure 9). However, the elemental concentration at the surface was considerably altered in both FZrC-BA and FZrC-BA+MDPS surfaces when compared with starting ZrC powders (Table 4). After the functionalization with BA, an increase was observed for the atomic percentage of C (from 46.9 to 58.7%). In parallel, O and Zr atoms were detected less with a diminution of 9.2% and 2.8%, respectively. Particularly, for FZrC-BA+MDPS, the surface was mainly composed of C (66.3 %), O (26.7 %) and Si (4.2%), with the smallest amount of Zr obtained up to this point (2.9 %). This evolution indicated that the shell surface was predominantly occupied by organosilane moiety.

Secondly, the TG–DTA and corresponding MS analyses were performed for the two samples (Figure 20).

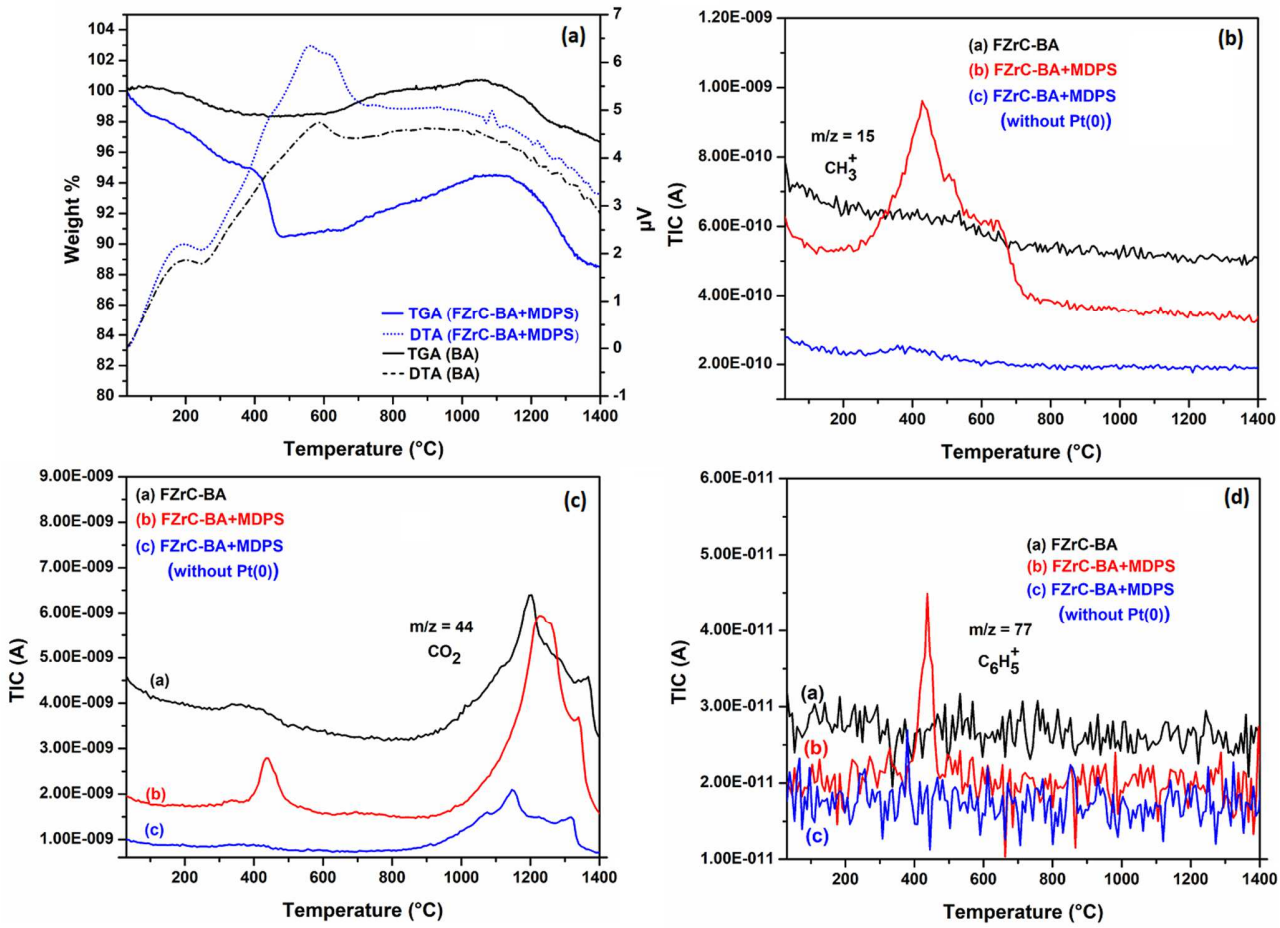


**Figure 20.** Thermal decomposition pattern of FZrC-BA and FZrC-BA+MDPS (a) base line corrected TG-DTA curves and gas evolution curves of various gaseous species (b) methyl ion, (c) carbondioxide & (d) phenyl ion.

The thermal behavior of the samples showed a first mass loss of ~9 % in the temperature range from 100°C to 450°C, in the case of FZrC-BA+MDPS. This event was more pronounced than for FZrC-BA (2 %),

in the same temperature range. According to the corresponding MS curves (Figure 20b-d), the major decomposition products were $CO_2$ (m/z=44) and $H_2$ (m/z=2) in both cases. Nevertheless, in addition to these events, methyl ion (m/z=15), phenyl ion (m/z=77) and traces of water were also detected in FZrC-BA+MDPS samples. Moreover, the obtained zeta potential value of FZrC-BA+MDPS (-39 mV) was far higher than FZrC-BA (-26 mV) and the suspension stability was found to be comparatively good. However, these results were not conclusive for the success of the hydrosilylation reaction. Hence, in order to verify the attachment of MDPS to the pendant alkene with a platinum catalyst, the hydrosilylation reaction was carried out without a Pt(0) catalyst. According to TG/DTA-MS analyses, the results displayed a comparable thermal decomposition pattern of FZrC-BA, but no methyl (m/z=15) or phenyl (m/z=77) ions species were observed. Thus, the hydrosilylation reaction leading to FZrC-BA+MDPS was validated for the functionalized ZrC surface, as the catalyst is necessary to perform this addition. Hence, the approach using first a complexation of zirconium then a hydrosilylation reaction between the alkene functional groups and the hydrogenosilane from MDPS, could lead to the attachment of macromolecules onto the ZrC surface. This efficient route, proved both by theoretical and experimental methods, could lead to a new hybrid material platform in the field of non-oxide ceramics, to access core-shell structures. The exact amount of surface coverage molecules still remained a scientific obstacle that will be thoroughly examined in our future work on this subject.

**4. Summary and conclusion**

DFT studies were performed on the functionalization of ZrC surfaces with further grafting of preceramic organic precursors with the aim of controlling the chemical process to synthesize ZrC core/SiC shell composites. This work was carried out on the exposed surface of $ZrO_2$ on a ZrC substrate, which was studied in a previous work. In the first part of the study, the exposed surface was modified with water. There was an adsorption of molecular water molecules at a wide range of pressures with hydroxyl groups appearing at extremely low water partial pressures. The resulting hydrated surface was further functionalized with ACDMS in a nucleophilic substitution reaction with the release of HCl gas. A rearrangement in the adsorbed molecular water to hydroxyl groups was theoretically observed when ACDMS was adsorbed, and the interaction of ACDMS with the OH groups was rather weak. However, further grafting of a polymeric precursor using a hydrosilylation reaction was a highly favorable exothermic reaction.

Due to the weak interaction between ACDMS and the hydroxyl groups on the surface, other alternatives were originally examined with different bifunctional organic molecules in which one functional group could be used to adsorb on the surface, and the other functional group used to react with ACDMS. Lactic acid, ethanoic acid, oxalic acid and 4-hydroxybenzoic acid were all tested. They all exhibited strong adsorption to the surface but the reaction with ACDMS was unfavorable and indicated the route of a nucleophilic substitution reaction using ACDMS as inappropriate for the intended goal. 3-butenoic acid was finally used to exploit the availability of a carboxylic acid for strong gripping to the surface through chelating effect of the two oxygen atoms, and a subsequent usage of the terminal alkene bond for the hydrosilylation reaction. This reagent gave excellent unprecedent results, both on theoretical and experimental aspects, with a favorable adsorption onto the surface and an exothermic hydrosilylation reaction in the grafting-to method with a molecule representative of the macromolecule (MDPS). These promising results showed the possibility of optimizing the interaction between organic molecules and an

inorganic surface of a non-oxide ceramic (ZrC). The generated hybrid systems could clearly represent a potential hybrid compound bank to ease the access to original core-shell systems.

**Acknowledgment**

The authors thank Miss Jessica Roper for her help in proofreading the manuscript. The project was also supported by the Agence Nationale de la Recherche under Contract No. ANR-12-BS08-004-02 (CollZSiC: Elaboration de nanocomposites coeur/coquille ZrC/SiC).

**References**


(1) D. Gosset, M. Dollé, D. Simeone, G. Baldinozzi, L. Thomé, Structural Evolution of Zirconium Carbide under Ion Irradiation, J. Nucl. Mater. 373 (2008) 123–129. https://doi.org/10.1016/j.jnucmat.2007.05.034.

(2) D. Gosset, M. Dollé, D. Simeone, G. Baldinozzi, L. Thomé, Structural Behaviour of Nearly Stoichiometric ZrC under Ion Irradiation, Nucl. Instrum. Meth. B 266 (2008) 2801–2805. https://doi.org/10.1016/j.nimb.2008.03.121.

(3) Y. Katoh, G. Vasudevamurthy, T. Nozawa, L. L. Snead, Properties of Zirconium Carbide for Nuclear Fuel Applications, J. Nucl. Mater. 441 (2013) 718–742. https://doi.org/10.1016/j.jnucmat.2013.05.037.

(4) G. H. Reynolds, J. C. Janvier, J. L. Kaae, J. P. Morlevat, Irradiation Behavior of Experimental Fuel Particles Containing Chemically Vapor Deposited Zirconium Carbide Coatings, J. Nucl. Mater. 62 (1976) 9–16. https://doi.org/10.1016/0022-3115(76)90279-8.

(5) K. Minato, T. Ogawa, K. Fukuda, H. Nabielek, H. Sekino, Y. Nozawa, I. Takahashi, Fission Product Release from ZrC-Coated Fuel Particles during Postirradiation Heating at 1600 °C, J. Nucl. Mater. 224 (1995), 85–92. https://doi.org/10.1016/0022-3115(95)00032-1.

(6) H. Li, L. Zhang, L. Cheng, Y. Wang, Oxidation Analysis of 2D C/ZrC–SiC Composites with Different Coating Structures in CH4 Combustion Gas Environment, Ceram. Int. 35 (2009) 2277–2282. http://dx.doi.org/10.1016/j.ceramint.2008.12.002.

(7) E. Osei-Agyemang, J. F. Paul, R. Lucas, S. Foucaud, S. Cristol, Oxidation and Equilibrium Morphology of Zirconium Carbide Low Index Surfaces Using DFT and Atomistic Thermodynamic Modeling. J. Phys. Chem. C 120 (2016) 8759–8771. https://doi.org/10.1021/acs.jpcc.6b01460.

(8) T. Noda, M. Yamazaki, K. Ozawa, K. Edamoto, S. Otani, Oxygen Adsorption on a ZrC(111) Surface: Angle-Resolved Photoemission Study. Surf. Sci. 450 (2000) 27–33. https://doi.org/10.1016/S0039-6028(99)01235-2.

(9) T. Noda, T. Nakane, K. Ozawa, K. Edamoto, S. Tanaka, S. Otani, Photoemission Study of the Oxidation of ZrC(111). Solid State Commun. 107 (1998) 145–148. https://doi.org/10.1016/S0038-1098(98)00189-6.

(10) A. Vojvodic, C. Ruberto, B. I. Lundqvist, Atomic and Molecular Adsorption on Transition-Metal Carbide (111) Surfaces from Density-Functional Theory: A Trend Study of Surface Electronic Factors, J. Condens. Matter Phys. 22 (2010) 375504. https://doi.org/10.1088/0953-8984/22/37/375504.

(11) K. Ozawa, T. Yoshii, T. Noda, K. Edamoto, S. Tanaka, Coadsorption of Oxygen and Cesium on ZrC(111), Surf. Sci. 511 (2002), 421–434. https://doi.org/10.1016/S0039-6028(02)01552-2.

(12) H. Kitaoka, K. Ozawa, K. Edamoto, S. Otani, The Interaction of Water with Oxygen-Modified ZrC(100) Surfaces. Solid State Commun. 118 (2001), 23–26. https://doi.org/10.1016/S0038-1098(01)00037-0.

(13) K. Shin, O. Ken-ichi, E. Kazuyuki, O. Shigeki, Photoelectron Spectroscopy Study of the Oxidation of ZrC(100). Jpn. J. Appl. 39 (2000) 5217.

(14) F. Viñes, C. Sousa, F. Illas, P. Liu, J. A. Rodriguez, Density Functional Study of the Adsorption of Atomic Oxygen on the (001) Surface of Early Transition-Metal Carbides, J. Phys. Chem. C 111 (2007) 1307–1314.

(15) J. A. Rodriguez, P. Liu, J. Gomes, K. Nakamura, F. Viñes, C. Sousa, F. Illas, Interaction of Oxygen with ZrC(001) and VC(001): Photoemission and First-Principles Studies, Phys. Rev. B Condens. Matter *72* (2005) 075427.
(16) F. Viñes, C. Sousa, F. Illas, P. Liu, J. A. Rodriguez, Systematic Density Functional Study of Molecular Oxygen Adsorption and Dissociation on the (001) Surface of Group IV-VI Transition Metal Carbides, J. Phys. Chem. C 111 (2007) 16982–16989.
(17) T. Shimada, K. Imamura, K. Edamoto, H. Orita, Electronic Structures of the Suboxide Films Formed on TiC(100) and ZrC(100) Surfaces: Density Functional Theory Studies, Surf. Sci. 603 **2009**, 2340–2344. https://doi.org/10.1016/j.susc.2009.05.018.
(18) S. Shimada, M. Inagaki, M. Suzuki, Microstructural Observation of the ZrC/ZrO2 Interface Formed by Oxidation of ZrC. J. Mater. Res. 11 (1996) 2594–2597. https://doi.org/10.1557/JMR.1996.0326.
(19) S. Shimada, M. Yoshimatsu, M. Inagaki, S. Otani, Formation and Characterization of Carbon at the ZrC/ZrO2 Interface by Oxidation of ZrC Single Crystals, Carbon 36 (1998) 1125–1131.
(20) Y. V. Miloserdin, K. V. Naboichenko, L. I. Laveikin, A. G. Bortsov, The High-Temperature Creep of Zirconium Carbide, Strength Mater *4* (1972), 302–305. https://doi.org/10.1007/BF01528408.
(21) G. A. Rama Rao, V. Venugopal, Kinetics and Mechanism of the Oxidation of ZrC, J. Alloy. Compd 206 (1994) 237–242. https://doi.org/10.1016/0925-8388(94)90042-6.
(22) S. Shimada, T. Ishi., Oxidation Kinetics of Zirconium Carbide at Relatively Low Temperatures, J. Am. Ceram. Soc 73 (1990), 2804-2808. https://doi.org/10.1111/j.1151-2916.1990.tb06678.x.
(23) R. W. Bartlett, M. E. Wadsworth, I.W. Cutler, Trans. Metall. Soc. 227 (1963).
(24) R. E. Bullock, J. L. Kaae, Performance of coated UO2 particles gettered with ZrC, J. Nucl. Mater. 115 (1983) 69–83. https://doi.org/10.1016/0022-3115(83)90344-6.
(25) S. Shimada Microstructural observation of ZrO2 scales formed by oxidation of ZrC single crystals with formation of carbon, Solid State Ion. 101-103 (1997) 749–753. https://doi.org/10.1016/S0167-2738(97)00326-3.
(26) M. Gendre, A. Maître, G. Trolliard, A Study of the Densification Mechanisms during Spark Plasma Sintering of Zirconium (Oxy-)Carbide Powders, Acta Mater. 58 (2010) 2598–2609. https://doi.org/10.1016/j.actamat.2009.12.046.
(27) A. W. Weimer, Carbide, Nitride and Boride Materials Synthesis and Processing, 80th ed.; Chapman and Hall, 1997.
(28) H. Li, L. Zhang, L. Cheng, Y. Wang, Z. Yu, M. Huang, H. Tu, H. Xia, Effect of the Polycarbosilane Structure on Its Final Ceramic Yield, J. Eur. Ceram. Soc. 28 (2008) 887–891. https://doi.org/10.1016/j.jeurceramsoc.2007.07.020.
(29) P. Greil, Polymer Derived Engineering Ceramics, Adv. Eng. Mater. 2 (2000) 339–348. https://doi.org/10.1002/1527-2648(200006)2:6<339::aid-adem339>3.0.co;2-k.
(30) E. Osei-Agyemang, J. F.Paul, R. Lucas, S. Foucaud, S. Cristol, Stability, Equilibrium Morphology and Hydration of ZrC(111) and (110) Surfaces with H2O: A Combined Periodic DFT and Atomistic Thermodynamic Study, Phys. Chem. Chem. Phys. 17 (2015), 21401–21413. https://doi.org/10.1039/c5cp03031e.
(31) E. Osei-Agyemang, J. F. Paul, R. Lucas, S. Foucaud, S. Cristol, Periodic DFT and Atomistic Thermodynamic Modeling of Reactivity of H2, O2, and H2O Molecules on Bare and Oxygen Modified ZrC (100) Surface, J. Phys. Chem. C 118 (2014) 12952-12961. https://doi.org/10.1021/jp503208n.
(32) D. Pizon, R. Lucas, S. Chehaidi, S. Foucaud, A. Maître, From Trimethylvinylsilane to ZrC–SiC Hybrid Materials, J. Eur. Ceram. Soc. 31 (2011) 2687–2690. https://doi.org/10.1016/j.jeurceramsoc.2010.12.014.

(33) D. Pizon, R. Lucas, S. Foucaud, A. Maître, ZrC□SiC Materials from the Polymer-Derived Ceramics Route, Adv. Eng. Mater. 13 (2011) 599–603. https://doi.org/10.1002/adem.201000336.
(34) J. Hafner Ab-Initio Simulations of Materials Using VASP: Density-Functional Theory and Beyond, J. Comput. Chem. 29 (2008), 2044–2078. https://doi.org/10.1002/jcc.21057.
(35) N. D. Mermin, Thermal Properties of the Inhomogeneous Electron Gas, Phys. Rev. 137 (1965) A1441–A1443. https://doi.org/10.1103/PhysRev.137.A1441.
(36) G. Kresse, D. Joubert, From Ultrasoft Pseudopotentials to the Projector Augmented-Wave Method, Phys. Rev. B 59 (1999) 1758–1775. https://doi.org/10.1103/PhysRevB.59.1758.
(37) J. P. Perdew, K. Burke, M. Ernzerhof, Generalized Gradient Approximation Made Simple, Phys. Rev. Lett. 77 (1996) 3865–3868. https://doi.org/10.1103/PhysRevLett.77.3865.
(38) M. Methfessel, A. T. Paxton, High-Precision Sampling for Brillouin-Zone Integration in Metals, Phys. Rev. B 40 (1989) 3616–3621. https://doi.org/10.1103/PhysRevB.40.3616.
(39) H. J. Monkhorst, J. D. Pack, Special Points for Brillouin-Zone Integrations, Physical Review B 13 (1976) 5188–5192. https://doi.org/10.1103/PhysRevB.13.5188.
(40) K. Reuter, M. Scheffler, First-Principles Atomistic Thermodynamics for Oxidation Catalysis: Surface Phase Diagrams and Catalytically Interesting Regions, Phys. Rev. Lett. 90 (2003) 461031–461034.
(41) M. Gendre, A. Maître, G. Trolliard, Synthesis of Zirconium Oxycarbide (ZrCxOy) Powders: Influence of Stoichiometry on Densification Kinetics during Spark Plasma Sintering and on Mechanical Properties, J. Eur. Ceram. Soc. 31 (2011) 2377–2385. https://doi.org/10.1016/j.jeurceramsoc.2011.05.037.
(42) A. Dasan, R. Lucas, E. Laborde, C. Piriou, S. Foucaud, Towards a Surface Functionalisation and Grafting of a Polycarbosilane onto Zirconium Carbide Particles for the Development of Hybrid Core-Shell Structures, Appl. Surf. Sci. 495 (2019) 143409. https://doi.org/10.1016/j.apsusc.2019.07.151.
(43) R. Lucas, D. Pizon, E. Laborde, G. Trolliard, S. Foucaud, A. Maître, A Simple Route for Organic Covalent Grafting onto Zirconium Carbide Particles, Appl. Surf. Sci. 287 (2013) 411–414. http://dx.doi.org/10.1016/j.apsusc.2013.09.170.
(44) D. L. Liao, G. S. Wu, B. Q. Liao, Zeta Potential of Shape-Controlled TiO2 Nanoparticles with Surfactants, Colloid surf. A - Physicochem. Eng. Asp. *348* (2009) 270–275. https://doi.org/10.1016/j.colsurfa.2009.07.036.
(45) F. Bouzat, A. R. Graff, R. Lucas, S. Foucaud, Preparation of C/SiC Ceramics Using a Preceramic Polycarbosilane Synthesized via Hydrosilylation, J. Eur. Ceram. Soc. 36 (2016) 2913–2921. https://doi.org/10.1016/j.jeurceramsoc.2015.11.032.
(46) K. L. Martin, D. P. Street, M. B. Dickerson, Polycarbosilane-Grafted Nanoparticles: Free-Flowing Hairy, Chem. Mater. *32* (2020) 3990-4001. https://doi.org/10.1021/acs.chemmater.0c00528
(47) C. De Dobbelaere, J. Mullens, A. Hardy, M. K. Van Bael, Thermal Decomposition and Spectroscopic Investigation of a New Aqueous Glycolato(-Peroxo) Ti(IV) Solution–Gel Precursor, Thermochim. Acta 520 (2011) 121–133. https://doi.org/10.1016/j.tca.2011.03.028.

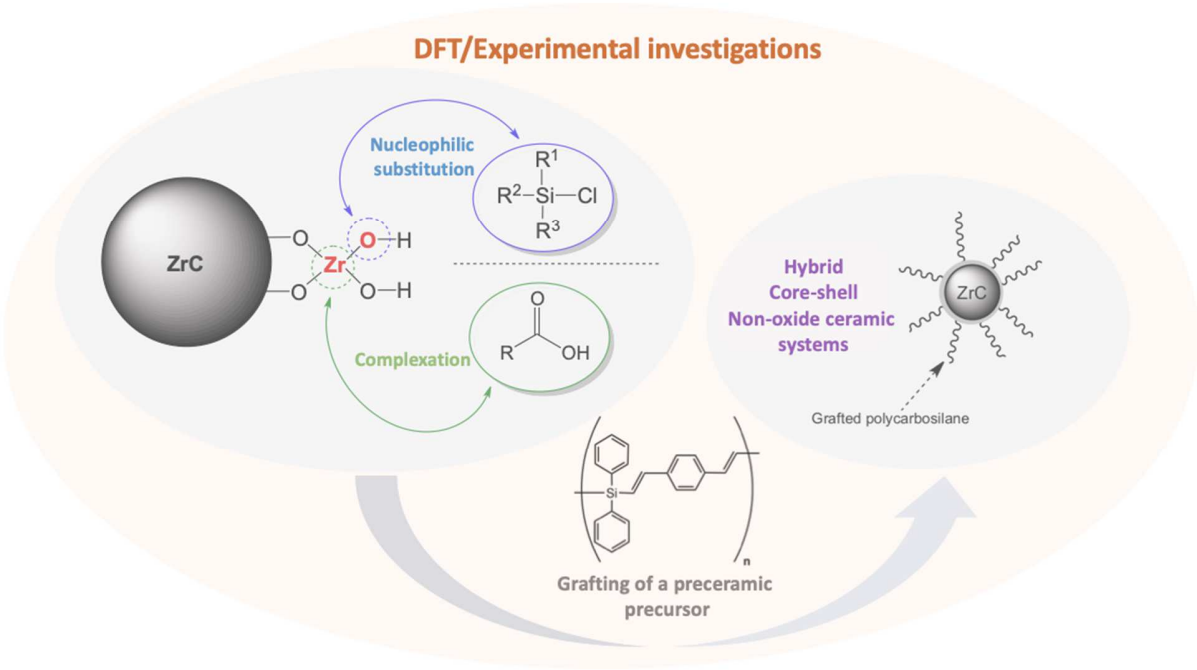
DFT/Experimental investigations
Nucleophilic substitution
ZrC
Zr
O—H
O—H
Complexation
Hybrid
Core-shell
Non-oxide ceramic
systems
ZrC
Grafted polycarbosilane
Grafting of a preceramic precursor